J. Opt. A: Pure Appl. Opt. **11** (2009) 045712 (8pp) doi:10.1088/1464-4258/11/4/045712

# Light propagation in 1D inhomogeneous deterministic media: the effect of discontinuities

**R Diamant and M Fernández-Guasti**[1]

Laboratorio de Óptica Cuántica, Departamento de Física, Universidad A. Metropolitana–Iztapalapa, Apartado postal. 55-534, 09340 México DF, Mexico

E-mail: ruth@xanum.uam.mx and mfg@xanum.uam.mx

Received 11 October 2008, accepted for publication 22 January 2009
Published 17 February 2009
Online at stacks.iop.org/JOptA/11/045712

**Abstract**
The propagation of light in one-dimensional inhomogeneous deterministic media where the refractive index varies on a wavelength scale is numerically evaluated without approximations. To this end, the field is written in amplitude and phase variables leading to a nonlinear amplitude differential equation. The numerical solutions to this Ermakov-type equation for five different refractive index profiles are presented. The amplitude oscillations are construed in terms of opposite phase or counter-propagating waves. The reflectivity is then evaluated for different interface thicknesses. The discontinuities in the first-and second-order derivatives are shown to produce an enhanced reflectivity even if the functions are continuous and monotonic.

**Keywords:** electromagnetic propagation, stratified media, reflectivity, discontinuity, atmospheric disturbances

(Some figures in this article are in colour only in the electronic version)

## 1. Introduction

The propagation of electromagnetic waves through inhomogeneous, deterministic, nonabsorbing media has been successfully described either when the permittivity variation takes place in a much larger or in a much shorter distance than the wavelength scale [1]. In the former limit, the amplitude derivatives are neglected on a wavelength scale leading to the eikonal equation [2 ch.3]. The ray equation is then solved analytically or numerically, depending on the complexity of the refractive index function. In the abrupt limit, Maxwell's equations are solved for each homogeneous medium with constant permittivity, say, $\varepsilon_1$ and $\varepsilon_2$. The wave solutions for each case are then joined at the interface by imposing the appropriate continuity conditions.

The intermediate case, where the refractive index varies on a wavelength scale, is more difficult to tackle [3, 4]. A few permittivity profiles allow for exact analytical solutions [5]. A useful strategy has been to solve the differential equations for a large number of thin homogeneous layers and then take the limit where the layers' permittivity approach the desired function; matrix methods are nicely suited to describe stratified or quasi-periodic media [6]. Another approach has been to build up an arbitrary profile through piecewise integration of simpler profiles that can be analytically solved [7]. Absorbing inhomogeneous layers have been addressed with various degrees of success [8, 9]. Recent efforts tackle the problem of anisotropic inhomogeneous media [10–12]. On the other hand, amplitude and phase methods have been successfully implemented in dynamical systems and quantum mechanics [13, 14] but are not so widespread in optics and electromagnetic propagation. The two variables can sometimes be decoupled: then nonlinear differential equations either for the amplitude or the phase are obtained. These equations have two advantages: on the one hand, the initial conditions can be readily enforced due, to some extent, to the precise physical meaning of the variables. On the other hand, iterative methods may be implemented in a straightforward way. Furthermore, at present, personal computers make full numerical calculations readily accessible [15]. Approximations can sometimes be avoided by using numerical methods to solve the associated differential equations with the desired degree of precision.

[1] http://investigacion.izt.uam.mx/mfg/

 © 2009 IOP Publishing Ltd Printed in the UK

The purpose of this paper is to exhibit the main reflectivity features that arise for different refractive index profiles, by solving numerically an Ermakov-type amplitude equation. Propagation is restricted to one dimension and normal incidence so that the refractive index variation is perpendicular to the polarization. The inhomogeneous media considered here are transparent and isotropic. The amplitude nonlinear differential equation is obtained from the amplitude and phase representation of the field in section 2. Analytical solutions for a constant refractive index are then presented in order to elucidate the nonlinear superposition principle for counter-propagating waves. In section 3, an interface thickness criterion is introduced together with the initial conditions that, as we shall see, is best to establish for the transmitted wave, i.e. final conditions rather than initial ones. The oscillatory behavior of the amplitude is related to the reflectivity. In section 4, different monotonic refractive index functions are proposed. Particular attention is given to permittivity profiles that are either continuous or have discontinuities in their first or second derivatives. The numerical solutions are presented in section 5 while the discussion and conclusions are drawn in section 6. Interference effects are observed even when the refractive index function and its first derivative are continuous. Reflections coming from the bulk as well as from the first-order or even second-order discontinuity planes are required to explain the reflectivity curves.

## 2. Mathematical formulation of the problem

Consider a transparent, nonmagnetic medium with a spatially dependent permittivity $\varepsilon = \varepsilon(z)$. Let an incident monochromatic electric wave field be polarized in the $\hat{e}_y$ direction and propagate in the $z$ direction. The wave equation obtained from Maxwell's equations is then [2, 16]

$$\frac{\partial^2 E_y}{\partial z^2} + \mu_0 \varepsilon(z) \omega^2 E_y = 0,$$

where $\omega$ is the frequency and $\mu_0$ the vacuum permeability. This second-order non-autonomous ODE is formally equivalent to the time-dependent harmonic oscillator differential equation [17]. The above equation may be rewritten as

$$\frac{\mathrm{d}^2 E_y}{\mathrm{d}z^2} + k_o^2 n^2 \, E_y = 0, \tag{1}$$

where the wavevector is $k_o = \sqrt{\omega^2 \mu \varepsilon_o}$ and the refractive index is $n = \sqrt{\frac{\varepsilon}{\varepsilon_o}}$. The solution to this differential equation is in general complex valued. The polar amplitude and phase complex representation may be written as $E_y(z) = A\mathrm{e}^{\mathrm{i}q}$, where $A$ and $q$ are real quantities that depend on $z$. Substitution in equation (1) yields

$$\frac{\mathrm{d}^2 A}{\mathrm{d}z^2} - A\left(\frac{\mathrm{d}q}{\mathrm{d}z}\right)^2 + 2\mathrm{i}\frac{\mathrm{d}A}{\mathrm{d}z}\frac{\mathrm{d}q}{\mathrm{d}z} + \mathrm{i}A\frac{\mathrm{d}^2 q}{\mathrm{d}z^2} = -n^2 k_o^2 A.$$

The real and imaginary parts of this equation are

$$\frac{\mathrm{d}^2 A}{\mathrm{d}z^2} - A\left(\frac{\mathrm{d}q}{\mathrm{d}z}\right)^2 = -n^2 k_o^2 A \tag{2}$$

$$2\mathrm{i}\frac{\mathrm{d}A}{\mathrm{d}z}\frac{\mathrm{d}q}{\mathrm{d}z} + \mathrm{i}A\frac{\mathrm{d}^2 q}{\mathrm{d}z^2} = 0. \tag{3}$$

Equation (3) can be readily integrated to obtain an invariant quantity given by

$$Q = A^2 \frac{\mathrm{d}q}{\mathrm{d}z}.$$

This exact invariant is closely related to the Ermakov–Lewis invariant. A nonlinear differential equation for the amplitude is obtained upon substitution of this result in equation (2):

$$\frac{\mathrm{d}^2 A}{\mathrm{d}z^2} - \frac{Q^2}{A^3} = -n^2 k_o^2 A.$$

This equation together with (1) form an Ermakov pair. These systems have received considerable interest in different fields [18, 19]. In order to obtain a dimensionless equation, allow the invariant to be equal to $Q = k_o A_o^2$, where $A_o$ is an initial amplitude. The dimensionless Ermakov equation is then

$$\frac{1}{k_o^2}\frac{\mathrm{d}^2 A_d}{\mathrm{d}z^2} - \frac{1}{A_d^3} = -n^2 A_d \tag{4}$$

where $A_d = A/A_o$ is now a dimensionless amplitude. Let the distance $z$ be measured in wavelength units, so that $k_0 = 2\pi$. This is the nonlinear amplitude ODE that is numerically solved for different refractive indices in this work.

### 2.1. Solutions for constant n

If the refractive index $n$ is constant, there are two possible solutions. The first one is the obvious particular solution with constant amplitude, say $A_1$, then the second derivative in (4) vanishes, leaving $A_d = \frac{1}{\sqrt{n}}$, which represents the amplitude of a wave traveling in one direction. However, if we have counter-propagating waves, a constant amplitude $A_d$ will not be enough to describe this case. The general solution is then required and may be obtained from the nonlinear superposition principle [20, 17]:

$$A_d = (A_1^2 + A_2^2 + 2A_1 A_2 \cos(2k_o n z - \beta))^{\frac{1}{2}}, \tag{5}$$

where $A_1$ and $A_2$ are the individual amplitudes of these counter-propagating waves and $\beta$ is a constant phase. Substitution of (5) in the nonlinear differential amplitude equation (4) shows that the constants $A_1$ and $A_2$ are not independent:

$$(A_1^2 - A_2^2)^2 = \frac{1}{n^2}. \tag{6}$$

The orthogonal functions invariant for two counter-propagating waves is [17]

$$Q = (A_1^2 - A_2^2)\frac{\mathrm{d}s}{\mathrm{d}z} + \left(A_2\frac{\mathrm{d}A_1}{\mathrm{d}z} - A_1\frac{\mathrm{d}A_2}{\mathrm{d}z}\right)\sin(2s). \tag{7}$$

In regions where the refractive index is constant, the phase becomes linear $2s = 2k_o n z - \beta$ and the opposite wave amplitudes are constant. The invariant is then

$$Q = (A_1^2 - A_2^2) k_o n. \tag{8}$$

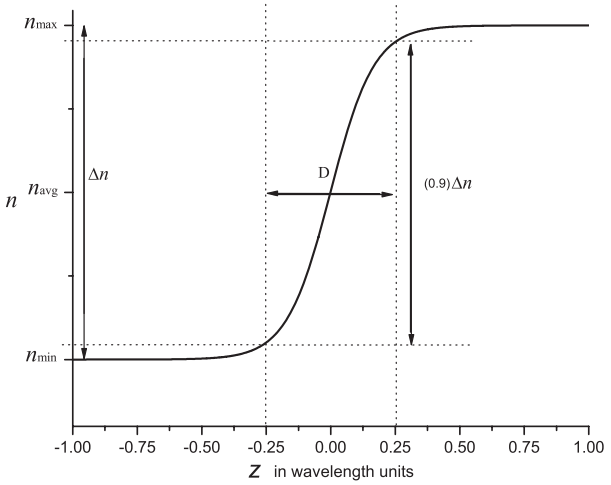


**Figure 1.** Typical distance $D$ (=0.5λ) defined as the region where 90% of the refractive index change takes place. The overall refractive index change is labeled $\Delta n$ and the half-value by $n_{avg}$.

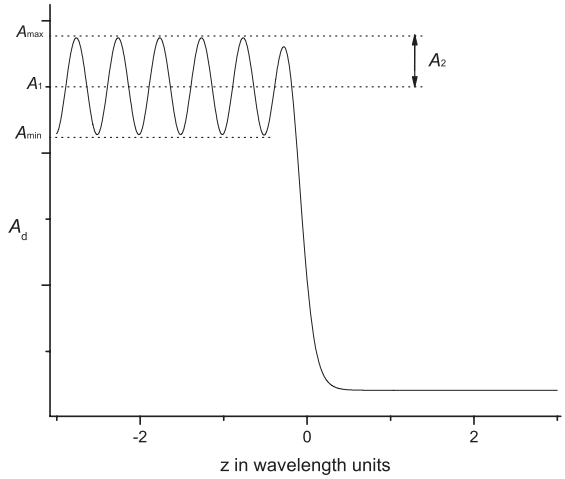


**Figure 2.** A typical graph for the wave amplitude $A_d$ obtained from the numerical solution to the differential equation (4). The refractive index used is a hyperbolic tangent function and the thickness is $D = 0.5$. Far away from the interface, $n$ is almost constant so the solution tends to $A_d = \frac{1}{\sqrt{n}}$ on the right ($z \gg 1$) and to (5) on the left ($z \ll -1$).

This result is equivalent to (6) since $Q = k_o A_o^2 = k_o$ for the dimensionless amplitude. The wave amplitudes far in the negative semi-space become the incident and reflected waves $A_1^2(-\infty) = A_{inc}^2$, $A_2^2(-\infty) = A_{ref}^2$. On the other hand, the amplitude far in the positive semi-space becomes the transmitted wave $A_1^2(\infty) = A_{trans}^2$ provided that $A_2^2(\infty) = 0$, that is, there is no incoming wave from the positive semi-space. If $n(-\infty) = n_{min}$ and $n(\infty) = n_{max}$

$$(A_{inc}^2 - A_{ref}^2) = \frac{1}{n_{min}}, \qquad A_{trans}^2 = \frac{1}{n_{max}}.$$

Equating these two expressions gives

$$(A_{inc}^2 - A_{ref}^2) n_{min} = A_{trans}^2 n_{max}.$$

This result exhibits the conservation of the electromagnetic energy flow.

## 3. Preamble for numerical approach

### *3.1. Interface thickness criterion*

A single inhomogeneous interface is modeled by $n(z)$ functions that change monotonically from $n_{min}$ when $z \to -\infty$ to $n_{max}$ when $z \to \infty$. In order to assess how fast the refractive index varies with $z$, a typical variation distance or maximum slope has to be established. Since many curves exhibit an asymptotic behavior the initial or final value may be attained at arbitrarily large distances. Nonetheless, a typical distance $D$ can be defined as the region where 90% of the refractive index change takes place, as shown in figure 1. This quantity $D$ is a measure of the interface thickness. The average refractive index and the difference between maximum and minimum values are defined as

$$n_{avg} = \frac{n_{max} + n_{min}}{2}, \qquad \Delta n = n_{max} - n_{min}. \tag{9}$$

In the numerical examples that follow, the gradual transition is considered to take place between, say, air and glass, that is $n_{min} = 1$ and $n_{max} = 1.5$. The difference between both indices is $\Delta n = 0.5$ and the mean refractive index is $n_{avg} = 1.25$.

### *3.2. Initial conditions*

It is customary to use the incident wave parameters as initial conditions. However, if a reflected wave is present, the plane where the incident wave is defined will also have a reflected wave, which is so far unknown. Furthermore, the interference of the counter-propagating incident and reflected waves produces a spatially varying amplitude whose slope at a given plane should also be stated.

In order to circumvent this problem it is more appropriate to establish the boundary conditions from the transmitted wave and then work the propagation backwards. Since there is no reflected wave far from the interface, the transmitted wave amplitude must be constant and its slope necessarily zero [16].

### *3.3. Evaluation of the reflectivity*

The numerical solution to the differential equation (1) establishes a field value for each position. This result does not show if the resultant field arises from the contribution of two or more fields. In other words, the solution does not distinguish the existence of an incident and a reflected wave but only its superposition. An equivalent assertion is true for the nonlinear amplitude equation (4) where an amplitude solution is found, regardless of whether it arises from the superposition of two fields.

Whenever the amplitude solutions exhibit time-independent oscillations, this behavior is considered to arise from the interference of two waves. A typical graph for $A_d$ from a previous work [16] is reproduced in figure 2.

The oscillations in the negative semi-space in the figure thus arise from counter-propagating incident $A_1$ and reflected $A_2$ wave amplitudes given by (5). These amplitudes in terms

**Table 1.** Refractive index profiles evaluated in the nonlinear amplitude differential equation (4).

| Label | $n(z)$ | Derivatives |
|---|---|---|
| *tanh* | $n_{\text{avg}} + \frac{\Delta n}{2}\tanh\left(\frac{2.94}{D}z\right)$ | All continuous |
| *arctan* | $n_{\text{avg}} + \frac{\Delta n}{\pi}\arctan\left(\frac{12.7}{D}z\right)$ | All continuous |
| *erf* | $1 + n_{\text{min}} + \frac{\Delta n}{2}\ \text{erf}\left(\frac{2.33}{D}z\right)$ | All continuous |
| *linear* | $\begin{cases} n_{\text{min}} & z \leqslant -\frac{D}{1.8} \\ n_{\text{avg}} + \frac{\Delta n}{2}(1.8\frac{z}{D}) & -\frac{D}{1.8} \leqslant z \leqslant \frac{D}{1.8} \\ n_{\text{max}} & z \geqslant \frac{D}{1.8} \end{cases}$ | All discontinuous |
| *cubic* | $\begin{cases} n_{\text{min}} & z \leqslant -\frac{D}{1.46} \\ n_{\text{avg}} + \frac{\Delta n}{2}(-1.55\frac{z^3}{D^3} + 2.19\frac{z}{D}) & -\frac{D}{1.46} \leqslant z \leqslant \frac{D}{1.46} \\ n_{\text{max}} & z \geqslant \frac{D}{1.46} \end{cases}$ | Only the first is continuous |

of the maxima and minima are $A_1 = \frac{A_{\text{max}}+A_{\text{min}}}{2}$ and $A_2 = \frac{A_{\text{max}}-A_{\text{min}}}{2}$. The intensity reflectivity coefficient is given by the quotient of the squared amplitudes

$$R = \left(\frac{A_2}{A_1}\right)^2 = \left(\frac{A_{\text{max}} - A_{\text{min}}}{A_{\text{max}} + A_{\text{min}}}\right)^2. \tag{10}$$

Since the second derivative of a function vanishes at the inflection points, the dimensionless amplitude from (4) becomes $A_d = \frac{1}{\sqrt{n_{\text{min}}}}$ at these points. Such inflections occur on the negative half-space where the oscillations take place as seen in figure 2. However, this value is not equal to $A_1$, the average of the maximum and minimum amplitudes on the negative half-space, where the oscillations take place.

## 4. Refractive index profiles

The nonlinear amplitude Ermakov equation is evaluated for five different refractive index profiles $n(z)$. The parameters of the refractive index curves have been set so that 90% of the variation takes place in an equal distance $D$ for all of them. The profiles are listed in table 1 and their graphs are shown in figure 3 for $D = 0.5$, that is, for an interface thickness of about half a wavelength. All the functions have been chosen to be symmetrical, invariant under a 180° rotation around an axis centered at $z = 0$, $n = n_{\text{avg}}$ and perpendicular to the plane in figure 1. Due to this symmetry and the equal $D$ criterion, all curves are coincident at $(z, n) = (-0.25, 1.025)$, $(0, 1.25)$ and $(0.25, 1.475)$, as may be seen in figure 3. The first profile '*tanh*' is based on a hyperbolic tangent function, the second one labeled '*arctan*' uses an inverse tangent function, whereas the third one involves an error function '*erf*' defined by $\text{erf}(x) = \frac{1}{\sqrt{\pi}}\int_{-\infty}^{x}\exp(-t^2)\,\text{d}t$. These first three functions are continuous and have continuous $n$th-order derivatives.

The last two functions are continuous piecewise functions. The '*linear*' function is constructed from three straight lines. The function derivatives are clearly discontinuous at the junctions. Finally, the '*cubic*' function is built up with a cubic polynomial pasted with two constant functions. The curves are joined at the points where the cubic curve has zero slope so that the first derivatives are also continuous.

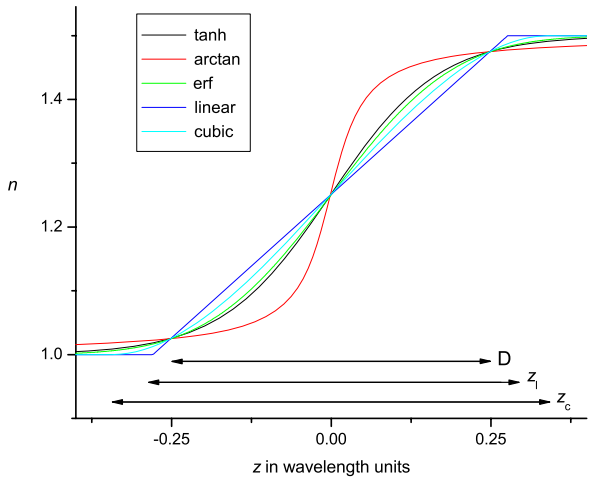


**Figure 3.** Refractive index profiles $n(z)$ that were used in the Ermakov amplitude equation. The profile functions are listed in table 1. The parameters of the curves have been set so that 90% of the variation takes place in an equal distance $D$ for all of them. The graph shown here corresponds to an interface thickness of half a wavelength $D = 0.5$ and refractive indices $n_{\text{min}} = 1$ and $n_{\text{max}} = 1.5$.

## 5. Numerical solutions

The nonlinear amplitude equation (4) is numerically solved for these five profiles. In each case, the differential equation is solved for 200 different interface thicknesses in the range $0.011 \leqslant D \leqslant 2.001$ in steps of 0.01. For a given differential equation, 4000 points are taken and the range of $z$ values depends on the interface thickness. Typical values for $D$ close to 2 are $-6 \leqslant z \leqslant 6$ whereas for $D$ less than unity $-2 \leqslant z \leqslant 2$. The important issue is to have values of $z$ sufficiently far away from the interface so that the oscillation's amplitude is constant.

The maxima and minima evaluated for each interface thickness far from the interface on the negative semi-space is recorded. The reflectivity is estimated from equation (10) based on this data. The reflectivity obtained in this way is plotted in figure 4 for all five different profiles. The plot involves the numerical evaluation of 1000 differential equations.

The reflectivity in the abrupt limit, as expected, is equal to the Fresnel reflection coefficient $R = (\frac{n_1-n_2}{n_1+n_2})^2$, regardless

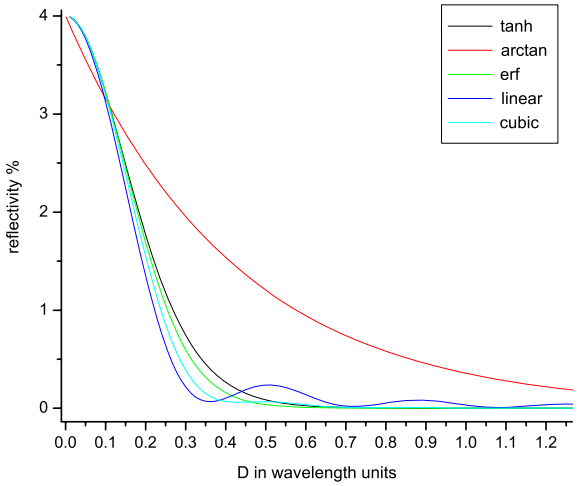


**Figure 4.** Reflectivity versus interface thickness $D$ for five different refractive index profiles. The reflectivity for each thickness is obtained from the numerical solution to the nonlinear amplitude equation (4) with the corresponding refractive indices given in table 1.

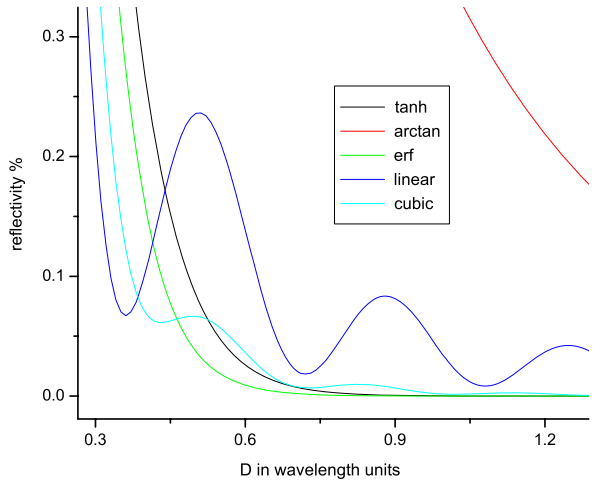


**Figure 5.** The oscillations in the reflectivity versus $D$ plot are due to discontinuous first and or second derivatives of the refractive index functions.

of the shape of the profile. All reflectivity curves approach the same reflectivity (4% in figure 4) as the thickness $D$ approaches zero.

In the opposite limit when the interface thickness is large, the reflectivity tends to zero for all profiles. This limit, of slowly varying refractive index function, produces negligible reflections just as predicted by the eikonal equation.

### 5.1. Tanh

The reflectivity for the '*tanh*' function can be fitted very well by

$$R = \frac{\sinh^2[a(n_{\max} - n_{\min})D]}{\sinh^2[a(n_{\max} + n_{\min})D]} \tag{11}$$

where $a = \frac{10}{3}$. This functional fit is proposed from the reflectivity function of an Epstein profile [5, 4]. The Epstein profile using our $D$ with 90% criterion is

$$n(z) = \sqrt{\frac{n_{\max}^2 + n_{\min}^2}{2} + \frac{n_{\max}^2 - n_{\min}^2}{2}\tanh\left(\frac{2.96}{D}z - 0.101\right)}.$$

This function is proportional to the square root of the tanh function used here. It should be noted that it is not symmetrical as the profiles chosen in this work. The Epstein profile makes the wave equation (1) analytically solvable via substitutions and using the hypergeometric series [5, 21]. The analytic solution for the reflectivity function is

$$R = \frac{\sinh^2\left[\frac{\pi k_0}{6}(n_{\max} - n_{\min})D\right]}{\sinh^2\left[\frac{\pi k_0}{6}(n_{\max} + n_{\min})D\right]}. \tag{12}$$

### 5.2. Arctan

The rate at which the reflectivity decreases is similar for all curves except for the inverse tangent function. The maximum slope or refractive index rate change for this curve is steeper than the rest as may be seen from figure 3. This feature then seems to depend more on the maximum gradient of the refractive index function rather than on the thickness criterion.

### 5.3. Erf

The reflectivity for the error function falls off monotonically more quickly than any of the other $C^\infty$ functions. It has the lowest reflectivity for thicknesses above $0.52D$, as may be seen from the amplified region plotted in figure 5. The error function has the smallest slope of the three $C^\infty$ functions consistent with the previous observation of the arc-tangent function that the reflectivity is related to the refractive index slope.

### 5.4. Discontinuous

The reflectivity for the last two functions show oscillations that are reminiscent of a thin film interference effect. Reflection from an interface is associated with the discontinuity of the refractive index function. Interference, as it is well known, is produced in a thin film due to the reflection at two planes where the refractive index is discontinuous. However, in the present case, all the refractive index profiles are continuous but oscillations as a function of thickness are only observed in the last two functions that have discontinuous derivatives. A closer look at these oscillations is shown in figure 5.

*5.4.1. Linear.* The first-order derivative of the *linear* function is discontinuous at $z = \pm D/1.8$ where the straight lines with different slopes meet. The distance between the discontinuities is $z_1 = \frac{2}{1.8}D \approx 1.11D$ as shown in figure 3. The minima and maxima in this linear case are evenly spaced as may be seen from table 2. However, the reflectivity decreases for each successive minimum. This behavior is expected since, for larger interface thicknesses, the function is softer and the reflectivity decreases.

Multiple beam interference is likely to originate from reflection at the first-order discontinuities (recall that the

**Table 2.** Local extrema for the linear and cubic reflectivity curves. The first column of the left is the number of the local minimum or maximum. The percentage intensity reflectivity is shown in the second column times 100. The third column shows the thickness $D$ where the minimum (or maximum) is attained. The column labeled $\Delta D$ shows the difference between the thickness $D$ of the $n$th + 1 minus $n$th minimum (or maximum). The averages of these quantities are shown at the bottom of the corresponding row.

| | *linear* | | | *cubic* | | |
|---|---|---|---|---|---|---|
| | Reflectivity (%) $\times 10^2$ | $D(\lambda_0)$ | $\Delta D$ | Reflectivity (%) $\times 10^2$ | $D(\lambda_0)$ | $\Delta D$ |
| | | Minima | | | Minima | |
| 1st | 6.71 | 0.36 | 0.36 | 6.14 | 0.43 | 0.30 |
| 2nd | 1.83 | 0.72 | 0.36 | 0.68 | 0.73 | 0.29 |
| 3rd | 0.83 | 1.08 | 0.36 | 0.15 | 1.02 | 0.29 |
| 4th | 0.47 | 1.44 | 0.36 | 0.05 | 1.31 | 0.29 |
| 5th | 0.30 | 1.80 | | 0.02 | 1.60 | |
| | | $\langle \Delta D \rangle_{\min} = 0.360$ | | | $\langle \Delta D \rangle_{\min} = 0.292$ | |
| | | Maxima | | | Maxima | |
| 1st | 23.64 | 0.51 | 0.37 | 6.67 | 0.49 | 0.34 |
| 2nd | 8.34 | 0.88 | 0.37 | 0.98 | 0.83 | 0.31 |
| 3rd | 4.23 | 1.25 | 0.36 | 0.27 | 1.14 | 0.29 |
| 4th | 2.56 | 1.61 | 0.36 | 0.11 | 1.43 | 0.30 |
| 5th | 1.71 | 1.97 | | 0.05 | 1.73 | |
| | | $\langle \Delta D \rangle_{\max} = 0.365$ | | | $\langle \Delta D \rangle_{\max} = 0.310$ | |

function itself is continuous). Following this hypothesis, the average thickness difference between the discontinuity planes for two adjacent minima is $\langle \Delta z_1 \rangle_{\min} = 1.11 \times 0.36 = 0.4$. The optical path is

$$\Lambda = \int n(z)\,\mathrm{d}z = \int_{-\frac{D}{1.8}}^{\frac{D}{1.8}} \left[ n_{\mathrm{avg}} + \frac{\Delta n}{2}\left(1.8\frac{z}{D}\right)\right]\mathrm{d}z = \frac{2}{1.8} D n_{\mathrm{avg}}.$$

The average optical path difference between two minima is

$$\langle \Delta\Lambda \rangle_{\min} = \frac{2}{1.8}\langle \Delta D \rangle_{\min} n_{\mathrm{avg}}.$$

For the present values $\langle \Delta D \rangle_{\min} = 0.36$ and $n_{\mathrm{avg}} = 1.25$, thus $\langle \Delta\Lambda \rangle_{\min} = 0.5$. This value of half a wavelength $\lambda/2$ is precisely what is expected for adjacent minima in thin film interference since the round trip is one wavelength. The optical path difference obtained from the maxima is $\langle \Delta\Lambda \rangle_{\max} = 0.507$, also very close to one-half. The maxima are shifted from the adjacent minima by $\Delta D_{\max-\min} = 0.15, 0.16, 0.17, 0.17, 0.17$, as may be seen from table 2. The optical path between adjacent max–min goes from $\Delta\Lambda_{\max-\min} = 0.21$ to 0.24, a range of values slightly under the 1/4 expected value.

The reflectivity for the linear profile resembles that of a hyperbolic profile studied by Jacobsson [4]. This profile joins two straight lines to a hyperbolic curve. None of the derivatives is continuous at the junctions as in the linear function considered here. An approximate fit proposed by Jacobsson for large wavenumbers is a sinc function squared.

*5.4.2. Cubic.* The *cubic* function is continuous in its first-order derivative since straight lines with zero slope are joined with the cubic polynomial at points $z = \mp D/1.46$, where the curve's derivative is also zero. However, the second-order derivative is discontinuous. The distance between the second-order discontinuities is $z_c = \frac{2}{1.46}D \approx 1.37D$. The average thickness difference between the discontinuity planes for two adjacent minima is $\langle \Delta z_c \rangle_{\min} = 1.37 \times 0.292 = 0.4$. The optical path is

$$\Lambda = \int_{-\frac{D}{1.37}}^{\frac{D}{1.37}} \left[ n_{\mathrm{avg}} + \frac{\Delta n}{2}\left(-1.55\frac{z^3}{D^3} + 2.19\frac{z}{D}\right)\right]\mathrm{d}z = \frac{2}{1.37} D n_{\mathrm{avg}}.$$

The average optical path difference between two minima is

$$\langle \Delta\Lambda \rangle_{\min} = \frac{2 \times 1.25}{1.37}\langle \Delta D \rangle_{\min} = 0.533,$$

a value just over the expected 1/2. The optical path difference obtained from the maxima is $\langle \Delta\Lambda \rangle_{\max} = 0.565$, that is a somewhat larger value compared with one-half. The maxima are shifted from the adjacent minima by $\Delta D_{\max-\min} = 0.06, 0.10, 0.12, 0.12, 0.13$. The thickness increase between maxima for higher-order max–min pairs that was mildly present in the linear function is now quite evident. The optical path goes from 0.11 to 0.24. The 0.25 path difference seems to be asymptotic for large orders. This attribute is reminiscent of the sinc or first-order Bessel function behavior in diffraction phenomena.

## 6. Discussion and conclusions

It is well established that:

- A reflected wave is produced when the refractive index varies as a function of position.
- If the refractive index variation takes place over large distances compared to the wavelength, the reflection coefficient becomes very small or negligible. In terms of the slope, a small refractive index slope (in wavelength

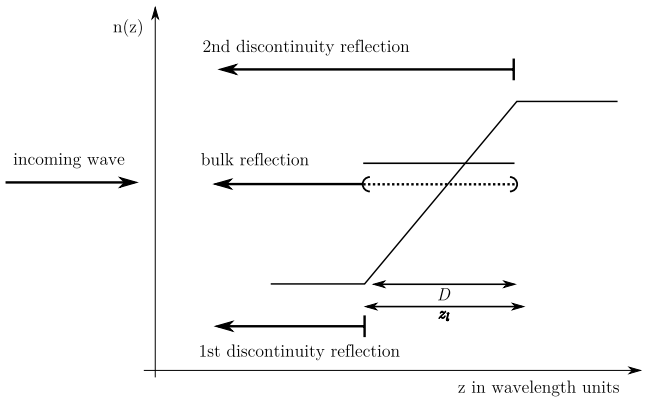


**Figure 6.** Contributions to the reflectivity for the linear profile. Bulk reflection arises from the region $z_l$ where the refractive index slope is finite. Two additional enhanced reflections arise at the planes where the function's first derivative is discontinuous.

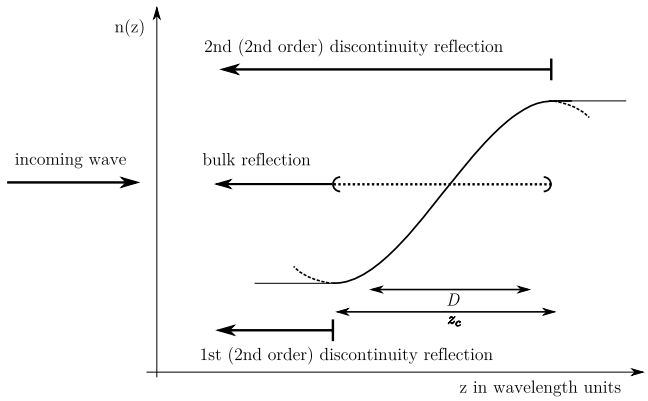


**Figure 7.** Contributions to the reflectivity for the cubic polynomial. Bulk reflection arises from the region $z_c$, where $n(z)$ is not constant. Two additional enhanced reflections arise at the planes where the function's second derivative is discontinuous although the function and its first derivative are continuous.

units), say of $\Delta n/2\lambda$ or smaller, produces a very small reflectivity even if the refractive index step $\Delta n$ is large.

- The reflectivity increases as the refractive index slope increases but approaches the abrupt limit around $\Delta n/\frac{1}{20}\lambda$. The abrupt limit is understood as a discontinuous function whose value, as well as that of its derivatives, change sharply as a function of position.

What is further asserted here is:

- a refractive index first-order discontinuity produces an enhanced reflected wave at the discontinuous plane even if the function itself is continuous;
- a refractive index second-order discontinuity produces an enhanced reflected wave at the discontinuous plane even if the function itself and its first derivative are continuous.

Let us see how these assertions explain the behavior of the reflectivity for the present profiles as well as others previously reported in the literature.

The reflectivity in the profiles with continuous derivatives comes from the bulk of the material where the refractive index slope varies rapidly. As the distance $D$ becomes smaller, the reflectivity increases monotonically. There is surely interference from the different planes within the bulk, but the smearing does not produce profile thicknesses $D$ where the interference is predominantly constructive or destructive.

In the linear profile, there are three distinctive contributions: (i) the reflectivity coming from the bulk where the refractive index has a finite linear slope as seen in figure 6. This contribution decreases monotonically with the slope decrease (large $D$). For this reason the minima in figure 5 are not zero for small $D$ but decrease rapidly for large thicknesses, as reported in table 2. (ii) There are enhanced reflectivities arising at the two well-defined planes where the function *derivative* is discontinuous. Depending on the separation between these planes, constructive or destructive interference produces maxima or minima in the reflectivity. The optical path between successive maxima or minima is indeed $\lambda/2$ ($\lambda$ round trip), thus strengthening this proposal.

The cubic profile again exhibits three characteristic contributions. (i) A contribution coming from the bulk where the refractive index has a large variation as a function of distance (finite slope) as seen in figure 7. It decreases monotonically for larger $D$. (ii) There must be enhanced reflectivities at the two planes where the second derivative is discontinuous. That is, the planes where the cubic polynomial is joined with the zero-slope straight lines. However, the reflectivity enhancement from the second-order discontinuity is smaller than the reflectivity arising from the first-order discontinuity as seen in figure 5. The interference of the waves coming from these two reflection planes exhibit less pronounced maxima and minima compared with the linear case. The optical path between successive maxima or minima is close to $\lambda/2$ ($\lambda$ round trip) although a slightly higher value is consistently obtained for the first few (lower-order) extrema.

To conclude, the reflectivity of a one-dimensional inhomogeneous deterministic medium may be efficiently evaluated from the nonlinear amplitude ODE numerical solutions. This procedure allows for the computation of the reflectivity even if the refractive index varies on the wavelength scale. The reflectivity curves as a function of interface thickness and profile shape have been explained in terms of the bulk reflectivity and increased reflectivities at the discontinuity planes. The discontinuities in the first-and second-order derivatives of the refractive index functions act as planes where the wave reflection is enhanced.

Thin film growth has become increasingly sophisticated. There is greater control over graded index layers and their combination with homogeneous thin or very thin layers. These structures may be analyzed using the present method with arbitrary precision, provided that the medium is continuous and transparent. An adequate refractive index gradient can diminish undesired reflections (anti-reflection coatings), enhance desired ones or act as a waveguide. Under different circumstances, no matter how smooth a thin film surface is, there is no perfectly sharp interface. Such is the case of oxide thin films used in mainstream electronics where polar and nonpolar layers intermingle [22]. The nonlinear amplitude numerical solutions described in this paper render an accurate description in these conditions when the boundaries are not sharp.

Optical methods used to characterize thin film structures ultimately rely on the reflectivity data. Oscillations in the reflectivity as a function of wavelength are usually interpreted in terms of wave interference between abrupt refractive index layers [23]. However, as shown here, such oscillations may also originate from continuous refractive index profiles provided that they exhibit discontinuous derivatives. Therefore, a refined interpretation of the oscillations is required in order to establish the nature of the discontinuity that produces the reflection enhancement.

Electromagnetic wave scattering and reflection from refractive index fluctuations in the clear air atmosphere have been of considerable interest. This information is used for remote sensing of atmospheric disturbances and density variations [24]. The method presented here may prove useful for a reassessment of the theoretical analysis of Doppler radar measurements. In the present method, neither the Fresnel nor Fraunhofer approximations are made. However, the price paid is a much simpler one-dimensional analysis at normal incidence. An appropriate generalization is required to tackle more complex two- or three-dimensional disturbances.

## References


[1] Fernández-Guasti M and Gil-Villegas A 1988 Propagation of rays in a duct with a radially variable refractive index: first integral solutions for Gaussian profiles *Opt. Commun.* **69** 105–7

[2] Born M and Wolf E 2005 *Principles of Optics* 7th edn (Cambridge: Cambridge University Press)

[3] Geffcken W 1941 Reflection elektromagnetischer wellen an einer inhomogenen schicht *Ann. Phys. Lpz.* **40** 385

[4] Jacobsson R 1966 Light reflection from films of continuously varying refractive index *Progress in Optics* vol V (Amsterdam: North-Holland) chapter V

[5] Epstein P S 1930 Reflection of waves in an inhomogeneous absorbing medium *Proc. Natl Acad. Sci.* **16** 627–37

[6] Abeles F 1950 Recherches sur la propagation des ondes electromagnetiques sinusoidales dans les milieux stratifie *Ann. Phys. Fr.* **5** 706–84

[7] Andrianov V A and Yushkova O V 1994 Mathematical model for calculation of reflection coefficient from dielectric inhomogeneous half-space *J. Commun. Technol. Electron* **39** 37–41

[8] Larruquert J I 2006 Reflectance optimization of inhomogeneous coatings with continuous variation of the complex refractive index *J. Opt. Soc. Am.* A **23** 99–107

[9] Abeles F and Theye M L 1966 Methode de calcul des constantes optiques des couches minces absorbantes a partir des mesures de reflexion et de transmission *Surf. Sci.* **5** 325–31

[10] Grafström S 2006 Reflectivity of a stratified half-space: the limit of weak inhomogeneity and anisotropy *J. Opt. A: Pure Appl. Opt.* **8** 134

[11] Cojocaru E 1997 Generalized Abeles relations for anisotropic thin film of an arbitrary dielectric tensor *Appl. Opt.* **36** 2825

[12] Doviak R J and Zrnic D S 1984 Reflection and scatter formula for anisotropically turbulent air *Radio Sci.* **19** 325–36

[13] Froman N 2002 *Physical Problems Solved by the Phase-Integral Method* (Cambridge: Cambridge University Press)

[14] Fernández-Guasti M and Moya Cessa H 2003 Amplitude and phase representation of quantum invariants for the time dependent harmonic oscillator *Phys. Rev.* A **67** 063803

[15] Jacobsson R 1993 Review of the optical properties of inhomogeneous thin films *Proc. SPIE* **2046** 2–8

[16] Fernández-Guasti M, Gil-Villegas A and Diamant R 2000 Ermakov equation arising from electromagnetic fields propagating in 1D *Rev. Mex. Fís.* **46** 530–5

[17] Fernández-Guasti M 2007 *Nonlinear Phenomena Research Perspectives* (NY: Nova Publishers) chapter 6 (The Nonlinear Amplitude Equation in Harmonic Phenomena) pp 177–223

[18] Haas F 2002 Generalized Hamiltonian structures for Ermakov systems *J. Phys. A: Math. Gen.* **35** 2925–35

[19] Fernández-Guasti M, Luis Jiménez J, Agustín F G and Cornejo-Rodríguez A 2003 Amplitude and phase representation of monochromatic fields in physical optics *J. Opt. Soc. Am.* A **20** 1629–34

[20] Reid J L and Ray J R 1980 Ermakov systems, nonlinear superposition and solutions of nonlinear equations of motion *J. Math. Phys.* **21** 1583–7

[21] Polyanin A D and Zaitsev V F 1995 *Handbook of Exact Solutions for Ordinary Differential Equations* (Boca Raton, FL: CRC Press)

[22] Nakagawa N, Hwang H Y and Miller D A 2006 Why some interfaces cannot be sharp *Nat. Mater.* **5** 204–9

[23] Goodman A M 1978 Optical interference method for the approximate determination of the refractive index and thickness of a transparent layer *Appl. Opt.* **17** 2779–87

[24] Muschinski A 2004 Local and global statistics of clear-air doppler radar signals *Radio Sci.* **39** RS1008–23